Low Temperature Electron Spin Resonance of the Kondo Ion in a Heavy Fermion Metal: $YbRh_2Si_2$

J. Sichelschmidt,[1] V. A. Ivanshin,[2] J. Ferstl,[1] C. Geibel,[1] and F. Steglich[1]

[1]*Max Planck Institute for Chemical Physics of Solids, D-01187 Dresden, Germany*

[2]*MRS Laboratory, Kazan State University, 420008 Kazan, Russia*

(Received 12 May 2003; published 6 October 2003)

We report an electron spin resonance (ESR) study on single crystals of the heavy fermion metal $YbRh_2Si_2$ which shows pronounced non-Fermi liquid behavior related to a close antiferromagnetic quantum critical point. It is shown that the observed ESR spectra can be ascribed to a bulk Yb^{3+} resonance. This is the first observation of ESR of the Kondo ion itself in a dense Kondo lattice system. The ESR signal occurs *below* the Kondo temperature (T_K) which thus indicates the existence of large unscreened Yb^{3+} moments *below* T_K. We observe the spin dynamics as well as the static magnetic properties of the Yb^{3+} spins to be consistent with the results of nuclear magnetic resonance and magnetic susceptibility.

DOI: 10.1103/PhysRevLett.91.156401 PACS numbers: 71.27.+a, 75.20.Hr, 76.30.–v

The heavy fermion compound $YbRh_2Si_2$ is located very close to a magnetic instability, related to the disappearance of antiferromagnetic (AF) order (due to increasing $4f$—conduction electron hybridization). Very weak AF order is observed at ambient pressure below the very low ordering temperature of $T_N \simeq 70$ mK. At $T > T_N$ pronounced deviations from the Landau Fermi liquid behavior are observed up to temperatures of $T \simeq 10$ K [1,2]. The magnetic response is highly anisotropic which indicates that the Yb^{3+} moments are forming an easy-plane square lattice perpendicular to the crystallographic c direction [1,2]. A tiny magnetic field of $B_c = 0.06$ T is sufficient to suppress the weak AF order [2] leading to a field-induced quantum critical point (QCP), $T_N \rightarrow 0$. Thus $YbRh_2Si_2$ has proven to be a favorable compound to investigate non-Fermi liquid (NFL) phenomena which are related to the proximity of a QCP. The effect of disorder on the NFL behavior may be neglected [1,2]. This is indicated by a low residual resistivity, $\rho_0 \approx 1\ \mu\Omega$ cm, of the single crystals and the homogeneity of the spin susceptibility, both static [^{29}Si nuclear magnetic resonance (NMR) Knight shift [3]] and dynamic (muon spin relaxation [4]). Two competing theoretical scenarios have been advanced to describe the heavy electron QCP: a spin density wave scenario [5,6] and a localized moment scenario [7]. In the former scenario magnetism develops by the spin polarization of the Fermi surface and NFL behavior results from the scattering of the quasiparticles by quantum critical spin fluctuations. The localized moment scenario assumes that heavy electrons are bound states between the local moments and conduction electrons which disintegrate at the QCP. In $YbRh_2Si_2$ the electron spin resonance (ESR) reported in this Letter proves the existence of localized moments down to the lowest accessible temperature of 1.5 K, i.e., substantially below the Kondo temperature $T_K \approx 25$ K [1], and therefore seems to favor the localized moment scenario in that system.

ESR probes the imaginary part of the dynamic susceptibility $\mathrm{Im}\chi(q = 0, \omega)$, and it is sensitive to the local electronic properties of the $4f$ ions. But, in typical ESR setups which use energies ≈ 0.04 meV, the Kondo ion in heavy fermion systems is not an appropriate ESR probe. This is due to the fact that the typical spin-fluctuation rate of the Kondo ions causes a large ESR linewidth which makes the ESR signal undetectable. Up to now a direct observation of the Kondo ion by ESR has been reported only in dilute Kondo alloys with an extremely small T_K. ESR of Yb^{3+} ions diluted in Au ($T_K \simeq 10\ \mu$K) [8] provided clear evidence for the Kondo effect in an ESR spectrum for $T_K \ll T < 1$ K. Much work has been done in the past on dense Kondo lattice systems with an additional ESR-probe ion (Gd^{3+} in most cases) [9–11]. This technique allowed detailed ESR investigations of the various ground-state properties in heavy fermion systems although the influence of the doped ESR probe to the Kondo lattice has to be taken into account. Since $T_K \approx 25$ K for $YbRh_2Si_2$ [1,2], one would not expect to observe any ESR below T_K in $YbRh_2Si_2$, because the linewidth is expected to be huge ($k_B T_K/\mu_B \approx 37$ T). The results presented here clearly refute this assumption. From the analysis of the observed ESR spectra of $YbRh_2Si_2$ it turns out that the ESR is probing the local Yb^{3+} $4f$ spins. Thus, this is the first-ever observation of ESR in a dense Kondo lattice system without additionally doped spin probes.

The ESR experiments were performed at frequencies 9.4 GHz (X band) and 34.1 GHz (Q band). We investigated five single crystalline platelets of $YbRh_2Si_2$ (thickness $\approx 100\ \mu$m, 2–4 mm^2 surface area). Their preparation as well as their magnetic and transport properties have been described elsewhere [1,2]. The high quality of the single crystals is evidenced by a residual resistivity ratio of $\rho_{300\,K}/\rho_0 \sim 68$ (≈ 20 times larger than in previous polycrystalline samples [1]), and a very sharp anomaly in the specific heat at $T = T_N$ [12] associated with an entropy release as low as $\approx 0.01 R\ln 2$, in

 © 2003 The American Physical Society

good agreement with the tiny ordered moment of $(10^{-3}–10^{-2})\mu_B/\mathrm{Yb}^{3+}$ [4].

ESR probes the absorbed power P of a transversal magnetic microwave field as a function of an external, static magnetic field B. Figure 1(a) shows two typical spectra which are recorded as dP/dB vs B. No hyperfine structure which may arise due to $^{171}\mathrm{Yb}$ and $^{173}\mathrm{Yb}$ was observable in the whole T region, likely due to the mechanism of a strong exchange narrowing of the ESR line. The asymmetry of the Lorentzian-type line shape is due to a nonvanishing dispersion contribution to the line and is typical for metallic samples where the penetration depth is smaller than the sample size [13]. The penetration depth of our crystals is $\approx 1\ \mu\mathrm{m}$. Therefore, we exclude the ESR signal being dominated by the sample surface, which is further established by the sample independence of the ESR parameters. We obtained excellent agreement between an asymmetric Lorentzian line [solid in Fig. 1(a)] and the experimental data. This enabled us to determine the ESR parameters resonance field B_{res} and linewidth ΔB to an accuracy of less than 0.3% (B_{res}) and 4% (ΔB) for $T \leq 20$ K.

In order to estimate the amount of Yb^{3+} ions which contribute to the ESR spectra we compared the ESR intensities of $\mathrm{YbRh_2Si_2}$ and the intermetallic compound $\mathrm{Y_{0.99}Yb_{0.01}Pd_3}$ which, due to its similar ESR parameters [14] and penetration depth, is well suited for such a comparison. Ensuring the same measuring conditions, we estimate that at least 60% of the Yb^{3+} ions in $\mathrm{YbRh_2Si_2}$ contribute to the observed ESR signal. This lower bound takes into account uncertainties which arise from (i) assuming comparable quality factors of the microwave cavity for both samples and from (ii) uncertainties in determining the sample size, mass, and penetration depth. Therefore, the observed ESR resonance is indeed a bulk property and cannot be ascribed to foreign Yb^{3+} phases.

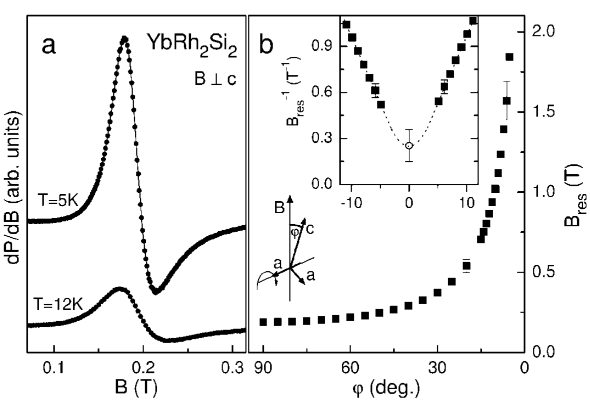

FIG. 1. (a) ESR spectra at 9.4 GHz (X band). Solid lines represent fits to the data with a Lorentzian line shape showing an asymmetry typical for metals. (b) Angle dependence of the resonance field B_{res} at $T = 5$ K. The single crystal is rotated in the magnetic field B as illustrated in the drawing. Inset: reciprocal B_{res} for $|\varphi| < 12°$. The dotted line is a guide to the eye that indicates the required vanishing of $dB_{\mathrm{res}}/d\varphi$ at $\varphi = 0°$. The bar yields uncertainty for $B_{\mathrm{res}}^{\|}(\varphi = 0°) \approx 4$ T.

The ESR intensity I_{ESR} reflects the uniform static susceptibility $\chi(q = 0)$ of the Yb^{3+} moments and is proportional to the area under the absorption signal. Its T dependence follows nicely a Curie-Weiss law with a negative Weiss temperature of $\Theta_\perp = -1.5$ K, indicating AF correlations. Similar behavior has been found for the bulk susceptibility as well [15]. We checked the direct correspondence of I_{ESR} and $\chi(q = 0)$ after measuring $\chi(q = 0)$ for B corresponding to the used X- and Q-band frequencies and at the $B \perp c$ axis. We found a linear relation $I_{\mathrm{ESR}} \propto (\chi - \chi_0)$, where $\chi_0 = (0.3 \pm 0.1) \times 10^{-6}\ \mathrm{m^3/mol\,K^2}$ denotes a small T independent contribution to the bulk susceptibility. χ_0 is related to the coefficient γ of the in-T linear specific heat by the Sommerfeld-Wilson ratio $R = (\chi_0/\gamma)(\pi^2 k_B^2/\mu_0\mu_{\mathrm{eff}}^2)$. Assuming $\mu_{\mathrm{eff}} = 1.4\mu_B$ and $\gamma \lesssim 0.5\ \mathrm{J/mol\,K^2}$ for $T > 1$ K [2], one gets $R \simeq 6$. A strongly enhanced Sommerfeld-Wilson ratio [2] has also been found using direct measurements of $\chi(q = 0)$ [2]. This was related to pronounced ferromagnetic (FM) fluctuations that have been observed in NMR measurements for fields above B_c [3].

B_{res} determines the ESR g factor via the resonance condition $\hbar\omega = g\mu_B B_{\mathrm{res}}$ and, therefore, reflects an effective g value of the ESR spin probe. In $\mathrm{YbRh_2Si_2}$ we identify the Yb^{3+} spin with a $^2F_{7/2}$ ground state as the ESR probe. To determine the proper crystal electric field (CEF) doublet ground state of Yb^{3+} we have analyzed the wave functions of the Kramers doublets with symmetries Γ_6 and Γ_7. Using the experimental g values and taking into account the g shift (discussed further below) the Γ_7 ground-state symmetry appears to be more likely to describe the g data than a Γ_6 ground state. A future publication will illustrate this topic in more detail.

$\mathrm{YbRh_2Si_2}$ displays a pronounced anisotropy of its magnetic properties which is related to the uniaxial symmetry of the Yb^{3+} environment. It manifests itself in a magnetic susceptibility which, when measured along the basal plane of the tetragonal structure, is almost 100 times larger than measured along the c axis at $T = 100$ mK [1]. Figure 1(b) shows that this strong magnetocrystalline anisotropy is imposingly reflected in a strong anisotropy of the resonance field giving further support for the bulk origin of the ESR signal. For the $B \perp c$ axis the resonance field at $T = 5$ K is $B_{\mathrm{res}}^{\perp} = (0.188 \pm 0.001)$ T which corresponds to $g_\perp = 3.561 \pm 0.006$. B_{res} strongly increases up to a nondetectable value when the c axis approaches the orientation parallel to B. The inset of Fig. 1(b) illustrates our estimation of $B_{\mathrm{res}}^{\|}$ corresponding to $g_\| = 0.17 \pm 0.07$. The values $g_\perp$ and $g_\|$ are comparable with those of the ESR of dilute Yb^{3+} dopant ions in the tetragonal system $\mathrm{PbMoO_4}$ [16], provided that a g shift of $\Delta g/g \simeq -8\%$ from the value of Yb^{3+} in an ionic environment is taken into account. In metals with a Pauli-like susceptibility the g shift contains a positive

(FM) local moment—conduction electron effective exchange integral $J_{\mathrm{eff}}(q=0)$ [17]. As shown in Fig. 2, Δg is negative in the whole T region. As discussed further below the negative value is due to the Kondo effect which causes an AF exchange, $J_{\mathrm{eff}}(q=0)<0$, between the conduction electrons and the Yb^{3+} spins.

$g(T)$ in Fig. 2 shows a T dependence very similar to the ^{29}Si NMR Knight shift data [3]. Thus, the observed ESR g factor seems to contain a g shift which, like the NMR Knight shift, is probing the spin susceptibility of $YbRh_2Si_2$. We have checked this assumption by plotting in the inset of Fig. 2 the $g_\perp$ values against the static bulk susceptibility ($\perp c$ axis), measured at magnetic fields which correspond to the low-T ESR resonance field. The plot proves that, within the experimental uncertainties, the $g_\perp$ values depend linearly on the static susceptibility. The slope is negative which, again, indicates an AF coupling. The slope of $g_\perp(\chi)$ depends on B, i.e., is smaller at 0.68 T (34.1 GHz) than at 0.19 T (9.4 GHz). This indicates a decreasing AF coupling with increasing B in accordance with the findings of the NMR that prove dominating FM fluctuations at $B>0.25$ T but, below $T=200$ mK and $B=0.15$ T, the emergence of critical AF fluctuations [3] which cause the NFL behavior in the vicinity of the QCP [2].

The solid line in the main part of Fig. 2 describes the g shift within a single-ion Kondo scenario which has been successfully applied to the ESR of Au:Yb [8]. There, a T-dependent effective exchange coupling [18] results in $\Delta g = c/\ln(\tilde{T}_K/T)$. Assuming $g^{\perp}_{\mathrm{ionic}}=3.86$ [16] the solid line corresponds to $c=1.67$ and $\tilde{T}_K=20$ mK. Taken $\tilde{T}_K$ as a characteristic spin-fluctuation temperature this value corresponds to a linewidth $\Delta B_K = k_B\tilde{T}_K/\mu_B \simeq 30$ mT which is in pretty good agreement with the observed linewidth. The small value of $\tilde{T}_K$ is consistent with the observation of very large unscreened Yb^{3+} moments ($\mu_{\mathrm{eff}} \simeq 1.4\mu_B$) in recent measurements of the $B=0$ static bulk susceptibility for $T_N<T<0.3$ K [15]. However, this low $\tilde{T}_K$ value differs by 3 orders of magnitude from the value which is derived from transport and thermodynamic properties of $YbRh_2Si_2$ determined at much higher temperatures ($T\approx 25$ K) [1,2]. This dramatic discrepancy cannot be explained yet. It either means that the magnetic properties require a quite different characteristic energy scale than transport and thermodynamic properties or, more likely, it is intimately related to the local nature of the QCP [7].

The nature of the relaxation mechanism of the Yb^{3+} spins is reflected by the linewidth ΔB which is measured as the half width at half maximum of the absorption $P(B)$. Its T dependence is shown in Fig. 3 for both used frequencies ($B\perp c$ axis). The dashed lines describe the linewidth data as follows. In the low T region ($T<12$ K) an increase linear in T fits $\Delta B(T)$ well with a slope $b=(3.1\pm 0.2)$ mT/K. Other Yb-doped intermetallics show comparable b values [19]. The linear behavior is typically found for a local moment relaxation in a metallic environment [13,17] where b is proportional to the squared exchange coupling of the local moments to the conduction electron spins. Above $T\simeq 12$ K an exponential increase $\Delta B(T) \propto 1/(\exp\frac{\Delta}{T}-1)$ becomes dominant with $\Delta \simeq 115$ K for both X- and Q-band data. This behavior is due to the modulation of the ligand field by lattice vibrations which cause, by means of spin-orbit coupling, a spin-lattice relaxation. In the case of acoustical vibrations CEF electronic states at an energy Δ above the ground state are involved in the relaxation, even for $T\ll\Delta$ ("Orbach-Aminov process") [20]. Also, optical vibrations may dominate the electron spin-lattice relaxation where optical phonons of energies $\hbar\omega \sim$

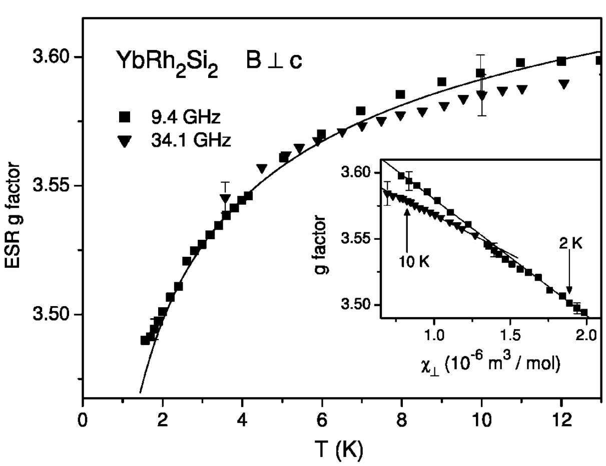

FIG. 2. T dependence of the effective g factor ($B\perp c$) at frequencies 9.4 GHz (0.19 T) and 34.1 GHz (0.68 T). The solid line describes the data with a logarithmic single-ion Kondo behavior. Inset: g factor vs the static bulk susceptibility $\chi_\perp$. Solid lines represent linear fits to the data.

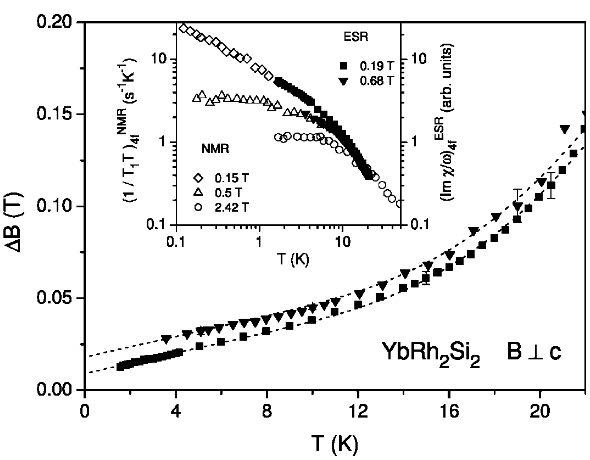

FIG. 3. T dependence of the ESR linewidth ΔB at frequencies 9.4 GHz (0.19 T, squares) and 34.1 GHz (0.68 T, triangles). Dashed lines represent the data as explained in the text. Inset: comparison of the ^{29}Si NMR $(1/T_1T)_{4f}(T)$ data (from Ref. [3], open symbols) with the T dependence of $(\mathrm{Im}\chi/\omega)^{\mathrm{ESR}}_{4f}$ obtained from the ESR data according to Eq. (1) (closed symbols).

Δ are involved [21,22]. The question whether optical or acoustical phonon relaxation processes dominate at high T will be the issue of a forthcoming publication. For $T \gtrsim 25$ K the ESR signal is too weak and too broad to be detected.

The ESR linewidth $\Delta B(T)$ contains valuable information on the dynamical magnetic properties as the nuclear spin relaxation rate $1/T_1(T)$ does in NMR. ESR is directly probing the damping Γ of the Yb^{3+} spin fluctuations at $q = 0$ via the ESR linewidth, $\Gamma = \omega_{ESR}\Delta B/B_{res}$, whereas the static Yb^{3+} spin susceptibility χ^0_{4f} is probed by the ESR intensity. Γ and χ^0_{4f} can be used for a comparison with the NMR data $(1/T_1T)_{4f}$ of the Yb^{3+} spins. According to the dissipation-fluctuation theorem $(1/T_1T)_{4f} \propto \mathrm{Im}\chi(\omega)_{4f}/\omega$; $(\hbar\omega/k_BT \ll 1)$. As a static B field is applied along a certain direction (z axis), $\chi(\omega)_{4f}$ consists of a longitudinal $\chi^{zz}_{4f}(\omega)$ and a transversal $\chi^{++}_{4f}(\omega)$ part. Using a purely relaxational ansatz one obtains a Lorentzian shape for $\mathrm{Im}\chi(\omega)_{4f}$, and the two components are written as

$$\frac{\mathrm{Im}\chi^{zz}_{4f}(\omega)}{\omega} = \chi^0_{4f} \cdot \frac{\Gamma}{\omega^2 + \Gamma^2} \quad \text{and}$$
$$\frac{\mathrm{Im}\chi^{++}_{4f}(\omega)}{\omega} = \chi^0_{4f} \cdot \frac{\Gamma}{(\omega - \omega_{4f})^2 + \Gamma^2}, \qquad (1)$$

where, because of the static B field, $\mathrm{Im}\chi^{++}_{4f}(\omega)$ is shifted by the Larmor frequency ω_{4f} of the Yb^{3+} spins taken at NMR magnetic fields B_{NMR}, $\omega_{4f} = \omega_{ESR}B_{NMR}/B_{res}$. The inset of Fig. 3 shows a comparison of the results of ^{29}Si NMR [3] with the sum of the above equations, denoted $[\mathrm{Im}\chi(\omega)/\omega]^{ESR}_{4f}$, where an NMR frequency $\omega/2\pi = 1.25$ MHz ($\equiv 0.15$ T) was used. Both ESR and NMR results show a change of slope below $T = 10$ K. This change gets more pronounced with increasing B. At fields 0.5 and 2.42 T, $(1/T_1T)^{NMR}_{4f}$ saturates at a constant value for sufficiently low T. This behavior is also indicated in $[\mathrm{Im}\chi(\omega)/\omega]^{ESR}_{4f}$ for the lowest accessible T at the Q-band field of 0.68 T. The saturation originates from a crossover from NFL to a field-induced Landau Fermi liquid regime, for which $1/T_1T$ is T independent [3]. At fields $B \leq 0.19$ T both ESR and NMR data do not show any saturation at low T. As mentioned before, for $(1/T_1T)^{NMR}_{4f}$ this fact was explained with developing critical AF ($q \neq 0$) spin fluctuations when approaching the Néel state ($B \rightarrow B_c^+$) [3].

From the analysis of the ESR in $YbRh_2Si_2$ described above it turns out that the observed resonance arises from local Yb^{3+} moments and that indeed the resonance is a bulk property. This is supported by (i) the resonance field anisotropy, which is in accordance with the strongly anisotropic magnetic susceptibility, (ii) the agreement of the observed g factors with those expected for $4f^{13}$ Yb^{3+}, and (iii) the linear relation between the g value, the intensity, and the static susceptibility. Therefore, our ESR results lead to the central conclusion that local magnetic Yb^{3+} moments exist well *below* the characteristic spin fluctuation or Kondo temperature characterizing consistently the thermodynamic and transport properties of $YbRh_2Si_2$ at higher temperatures. The existence of a well-behaved ESR line of Yb^{3+} at such low T indicates a lack of Kondo screening of the Yb^{3+} magnetic moments. Furthermore, from the field dependence of the ESR relaxation rate (see the inset of Fig. 3) as well as from the analysis of the ESR intensity we found evidence of dominating FM fluctuations above the critical field B_c, consistent with ^{29}Si NMR results [3].

From our results it is obvious that a simple single-ion Kondo scenario fails to explain our observations. On the other hand, the localized moment scenario for heavy fermion QCPs implies a type of dynamical susceptibility which relates to local critical degrees of freedom coexisting with spatially extended ones [7]. Such a scenario appears to be strongly supported by our observation that in $YbRh_2Si_2$ a well-behaved ESR signal due to local Yb^{3+} moments develops significantly below the ordinary Kondo temperature.

We acknowledge fruitful discussions with Hans-Albrecht Krug von Nidda, Philipp Gegenwart, and Oliver Stockert.

[1] O. Trovarelli *et al.*, Phys. Rev. Lett. **85**, 626 (2000).
[2] P. Gegenwart *et al.*, Phys. Rev. Lett. **89**, 056402 (2002).
[3] K. Ishida *et al.*, Phys. Rev. Lett. **89**, 107202 (2002).
[4] K. Ishida *et al.*, Physica (Amsterdam) **326B**, 403 (2003).
[5] A. J. Millis, Phys. Rev. B **48**, 7183 (1993).
[6] T. Moriya and T. Takimoto, J. Phys. Soc. Jpn. **64**, 960 (1995).
[7] Q. Si *et al.*, Nature (London) **413**, 804 (2001).
[8] K. Baberschke and E. Tsang, Phys. Rev. Lett. **45**, 1512 (1980).
[9] B. Elschner and A. Loidl, in *Handbook on the Physics and Chemistry of Rare Earths*, Vol. 24, edited by K. A. Gschneidner, Jr. and L. Eyring (Elsevier Science B.V., Amsterdam, 1997), Chap. 162.
[10] H.-A. Krug von Nidda *et al.*, Phys. Rev. B **57**, 14 344 (1998).
[11] S. Mair *et al.*, Phys. Rev. B **60**, 16 409 (1999).
[12] J. Custers *et al.*, Acta Phys. Pol. B **32**, 3211 (2001).
[13] S. E. Barnes, Adv. Phys. **30**, 801 (1981).
[14] C. Rettori *et al.*, Solid State Commun. **39**, 1025 (1981).
[15] P. Gegenwart *et al.*, Acta Phys. Pol. B **34**, 323 (2003).
[16] I. N. Kurkin and L. Ya. Shekun, Opt. Spectrosc. (USSR) **18**, 738 (1965).
[17] R. H. Taylor, Adv. Phys. **24**, 681 (1975).
[18] H. J. Spencer and S. Doniach, Phys. Rev. Lett. **18**, 994 (1967).
[19] T. Gambke *et al.*, J. Magn. Magn. Mater. **36**, 115 (1983).
[20] R. Orbach, Proc. R. Soc. London A **264**, 458 (1961).
[21] C. Huang, Phys. Rev. **154**, 215 (1967).
[22] V. A. Ivanshin, I. N. Kurkin, and G. Völkel, Phys. Status Solidi B **148**, K61 (1988).